J. Fluid Mech. (1974), *vol.* 63, *part* 1, *pp.* 145–156
Printed in Great Britain

Turbulent hypersonic viscous interaction

By J. L. STOLLERY† AND L. BATES
Department of Aeronautics, Imperial College, London

(Received 29 May 1973)

A theoretical analysis has been made of turbulent viscous interaction on isothermal surfaces at hypersonic speeds. The important parameters governing the effects of incidence and displacement have been obtained under both strong and weak interaction conditions for flat-plate flows. A more general expression relating boundary-layer growth to the external pressure field and effective body shape has been obtained. The method is applied to the wedge compression corner problem and the results compared with some experimental data.

1. Introduction

Viscous interaction describes flows in which the boundary-layer growth significantly distorts the external flow field, which in turn reacts on the development of the boundary layer. The effective body shape and the actual pressure distribution can differ widely from the geometric body shape and the inviscid pressure distribution so often used for boundary-layer calculations in subsonic and supersonic flows. There are a number of examples of viscous interaction throughout the Mach number range but two of the most important concern hypersonic flow near the sharp leading edge of a flat plate and shock–boundary-layer interaction.

As Barnes & Tang (1966) pointed out the leading-edge flow is unlikely to be turbulent since transition Reynolds numbers are so high at hypersonic speeds. However, shock–boundary-layer interaction in turbulent flow is certainly important and turbulent interaction on curved surfaces may also be of practical interest.

After the intuitive approach as outlined in, for example, the book by Hayes & Probstein (1959), the classic paper by Cheng *et al.* (1961) laid the foundations of laminar hypersonic viscous interaction. They uncovered the important parameters governing the flow and applied their analysis to a variety of inclined flat plates. Their work was later modified by Sullivan (1970) and extended to a wide range of curved surfaces by Stollery (1970). In this paper an attempt is made to provide a similar theory for turbulent flow. The greatest difficulty lies in adequately (and simply) expressing the growth of a turbulent boundary layer in terms of an initially unknown pressure distribution $P(x)$. Here the authors have initially adopted the intuitive approach which has proved so useful under laminar conditions for suggesting the relevant flow parameters and then adapted the momentum-integral method of Spence (1961) for a more detailed prediction method. Comparisons are made between such predictions and the experimental data of Coleman (1973) and Elfstrom (1972).

† Present address: College of Aeronautics, Cranfield Institute of Technology, Cranfield, Bedford, England.

2. Theory

Basically the problem is to find a solution to the set of equations

$$P = f_1(y_e), \quad y_e = f_2(\delta^*), \quad \delta^* = f_3(P), \qquad (1), (2), (3)$$

where P is the initially unknown pressure distribution $p_e(x)/p_\infty$, y_e is the effective body shape and δ^* is the boundary-layer displacement thickness. The pressure is assumed constant across the boundary layer, so that $p_e = p_w$. Equations (1)–(3) represent a very general statement of the problem. The functionally correct forms are given later.

Stollery (1970) showed that the Newton–Busemann pressure law as used by Cheng grossly overestimated the centrifugal effects for some curved surfaces and overall the tangent-wedge rule was the most satisfactory. Here we shall use either the tangent-wedge rule

$$P = 1 + \gamma K^2 \left[\frac{\gamma+1}{4} + \left\{\left(\frac{\gamma+1}{4}\right)^2 + \frac{1}{K^2}\right\}^{\frac{1}{2}}\right], \qquad (1a)$$

where $K = M_\infty dy_e/dx$, or the 'strong' and 'weak' approximations to it, i.e.

$$K^2 \gg 1, \quad P \simeq \tfrac{1}{2}\gamma(\gamma+1)K^2, \qquad (1b)$$

$$K \ll 1, \quad P = 1 + \gamma K. \qquad (1c)$$

The effective shape is taken as the displacement surface defined by

$$y_e = y_w + \delta^*, \qquad (2a)$$

where the geometric body shape $y_w(x)$ is given.

2.1. *The displacement thickness*

The simplest approach follows the intuitive method used to find the viscous interaction parameters for laminar flow. We extend the semi-empirical incompressible relations for turbulent flow over a flat plate† by writing

$$\frac{\delta^*}{x} \sim (\overline{Re}_x)^{-\frac{1}{5}} \sim \left\{\frac{\bar{\mu}}{\bar{\rho} u x}\right\}^{\frac{1}{5}} \sim \left\{\frac{\bar{\mu}}{\mu_\infty}\frac{\rho_\infty}{\bar{\rho}}\frac{1}{Re_x}\right\}^{\frac{1}{5}}, \qquad (3a)$$

where a bar denotes an average value in the boundary layer. Using the equation of state ($p = \rho RT$) together with the linear viscosity law

$$\bar{\mu}/\mu_\infty = C_\infty \bar{T}/T_\infty, \qquad (4)$$

equation (3 a) may be written as

$$\frac{\delta^*}{x} \sim Re_x^{-\frac{1}{5}}\left\{C_\infty \left(\frac{\bar{T}}{T_\infty}\right)^2 \frac{1}{P}\right\}.$$

Finally writing $\bar{T}/T_\infty \sim M_\infty^2$ (5)

we obtain $\delta^*/x \sim Re_x^{-\frac{1}{5}}\{C_\infty M_\infty^4/P\}^{\frac{1}{5}}$. (3 b)

This type of analysis is really only suitable for flat-plate flows where sensible average values can be specified. Before discarding (3 b) the strong and weak interaction parameters can be found and some simple examples considered.

† See, for example, the book by Duncan, Thom & Young (1970).

2.2. *The turbulent viscous interaction parameters*

If $y_w = 0$ then $y_e = \delta^*$ and $y'_e = d\delta^*/dx$, so that from (3 *b*)

$$M_\infty d\delta^*/dx \sim \{C_\infty M_\infty^9/Re_x P\}^{\frac{1}{5}}.$$

Hence for strong viscous interaction [equation (1 *b*)]

$$P \sim [C_\infty M_\infty^9/Re_x]^{\frac{2}{7}} \equiv \overline{\chi}_s. \tag{6}$$

For weak viscous interaction

$$P = 1+\gamma M_\infty(d\delta^*/dx) \simeq 1,$$

hence
$$M_\infty d\delta^*/dx \sim [C_\infty M_\infty^9/Re_x]^{\frac{1}{5}} \equiv \overline{\chi}_w. \tag{7}$$

The flat plate at incidence α. The above parameters are the same as those deduced by Barnes & Tang (1966) and suggest scalings for the characteristic equation for turbulent interaction obtained by combining (1 *a*), (2 *a*) and (3 *b*), namely

$$(y_e-y_w)\left\{1+\gamma M_\infty^2 y_e'^2\left[\frac{\gamma+1}{4}+\left\{\left(\frac{\gamma+1}{4}\right)^2+\frac{1}{M_\infty^2 y_e'^2}\right\}^{\frac{1}{2}}\right]\right\}^{\frac{1}{5}} = a_1 x\left\{\frac{C_\infty M_\infty^4}{Re_x}\right\}^{\frac{1}{5}}, \tag{8}$$

where a_1 is a constant. We attempt to scale this general equation using the weak interaction parameters $M_\infty\alpha$ and $\overline{\chi}_w$ since the most general form of the pressure relation (1 *a*) is a function of $M_\infty\alpha$, not just of $M_\infty^2\alpha^2$. Thus we write

$$Y = y/\alpha l, \quad X = x/l,$$

where
$$l = x\frac{M_\infty^9 C_\infty/Re_x}{M_\infty^5\alpha^5},$$

i.e.
$$X = \{M_\infty\alpha/\overline{\chi}_w\}^5.$$

The scaled equation is

$$(Y_e-Y_w)\left\{1+\gamma M_\infty^2\alpha^2 Y_e'^2\left[\frac{\gamma+1}{4}+\left\{\left(\frac{\gamma+1}{4}\right)^2+\frac{1}{M_\infty^2\alpha^2 Y_e'^2}\right\}^{\frac{1}{2}}\right]\right\}^{\frac{1}{5}} = a_1 X^{\frac{4}{5}} = a_1\left\{\frac{M_\infty\alpha}{\overline{\chi}_w}\right\}^4, \tag{9}$$

which confirms the important parameters, $M_\infty\alpha$ controlling the effect of incidence and $\overline{\chi}_w$ describing the displacement effect.

For strong interaction the simpler expression (1 *b*) may be used for P so that

$$(y_e-y_w)\,[\tfrac{1}{2}\gamma(\gamma+1)\,M_\infty^2 y_e'^2]^{\frac{1}{5}} = a_1 x\{C_\infty M_\infty^4/Re_x\}^{\frac{1}{5}} \tag{10}$$

replaces (8). The appropriate scaling is again

$$Y = y/\alpha l, \quad X = x/l,$$

but l is now
$$l = x\,\frac{M_\infty^9 C_\infty/Re_x}{M_\infty^7\alpha^7},$$

i.e.
$$X = \{M_\infty^2\alpha^2/\overline{\chi}_s\}^{\frac{7}{2}}.$$

The scaled equation is

$$(Y_e-Y_w)\,Y_e'^{\frac{2}{5}} = a_2 X^{\frac{4}{5}} = a_2\{M_\infty^2\alpha^2/\overline{\chi}_s\}^{\frac{14}{5}}, \tag{11}$$

where $a_2 = a_1/\{\frac{1}{2}\gamma(\gamma+1)\}^{\frac{1}{5}}$. Thus in this situation the single parameter is the ratio of the 'strong' inviscid term $M_\infty^2\alpha^2$ to the strong displacement term $\overline{\chi}_s$.

2.3. *The heat-transfer-rate distribution*

Heat-transfer (and skin-friction) relations can be found using an approach similar to that adopted by Eckert (1956) and others in the reference enthalpy methods, but consistent with the simple analysis described in §2.1. By analogy with the incompressible flow relation we write

$$St \equiv \frac{\dot{q}}{\bar{\rho} u_\infty (h_r - h_w)} \sim \left\{\frac{\bar{\rho} u_\infty x}{\bar{\mu}}\right\}^{-\frac{1}{5}}, \tag{12}$$

where bars again denote average properties in the boundary layer (it is tacitly assumed that $\bar{u} \simeq u_\infty$). Then

$$\begin{aligned} St_\infty \equiv \frac{\dot{q}}{\rho_\infty u_\infty (h_r - h_w)} &\sim \left(\frac{\bar{\rho}}{\rho_\infty}\right)^{\frac{4}{5}} \left(\frac{\bar{\mu}}{\mu_\infty}\right)^{\frac{1}{5}} Re_x^{-\frac{1}{5}} \\ &\sim P^{\frac{4}{5}} \left(\frac{\bar{T}}{T_\infty}\right)^{-\frac{4}{5}} \left(C_\infty \frac{\bar{T}}{T_\infty}\right)^{\frac{1}{5}} Re_x^{-\frac{1}{5}} \\ &\sim P^{\frac{4}{5}} C_\infty^{\frac{1}{5}} M_\infty^{-\frac{6}{5}} Re_x^{-\frac{1}{5}}, \end{aligned}$$

using (5). Hence

$$M_\infty^3 St_\infty \sim \{M_\infty^9 C_\infty / Re_x\}^{\frac{1}{5}} P^{\frac{4}{5}}. \tag{13}$$

For weak interaction $P \simeq 1$, so that

$$M_\infty^3 St_\infty \sim \bar{\chi}_w, \tag{14}$$

whereas for strong interaction $P \sim \bar{\chi}_s$, which gives

$$\begin{aligned} M_\infty^3 St_\infty &\sim \{M_\infty^9 C_\infty / Re_x\}^{\frac{1}{5}+\frac{4}{5}\times\frac{2}{7}} \\ &\sim \bar{\chi}_s^{\frac{3}{2}}. \end{aligned} \tag{15}$$

So far the simple relations have been based on expressions such as (3 *a*) and (3 *b*) suitable primarily for flat-plate flows. For more general surfaces it is important to find a more accurate relation for $\delta^*(x)$.

2.4. *A general expression for the displacement thickness*

The variation of δ^* with the pressure gradient, wall temperature ratio, Reynolds number and Mach number (provided that $M \gg 1$) can be found by adapting the analysis of Spence (1961). The somewhat sweeping assumption is made that for hypersonic flow the effective surface conditions (denoted by the subscript e) can be related to each other and to the free-stream conditions by the isentropic relations. The isentropic assumption is already implicit in writing the momentum equation in the form derived by Young (1953) as

$$\frac{d\theta}{dx} + (H + 2 - M_e^2) \frac{\theta}{u_e} \frac{du_e}{dx} = \frac{\tau_w}{\rho_e u_e^2}, \tag{16}$$

where θ is the momentum thickness, H the form factor δ^*/θ and τ_w the shear stress at the wall. Now

$$\frac{1}{u_e} \frac{du_e}{dx} = \frac{1}{M_e} \frac{dM_e}{dx} \left(1 + \frac{\gamma - 1}{2} M_e^2\right)^{-1}, \tag{17}$$

and for $M_e \gg 1$ and assuming Crocco's temperature relation the form factor can be written (see Spence 1961) as

$$H \simeq \frac{\gamma-1}{2} M_e^2 \left\{1 + H_i \frac{T_w}{T_0}\right\}, \tag{18}$$

where H_i is the incompressible value of H, T_w is the wall temperature and T_0 is the free-stream total temperature. Thus at hypersonic Mach numbers the momentum integral equation for a diatomic perfect gas ($\gamma = 1{\cdot}4$) is

$$\frac{d\theta}{dx} + \left\{H_i\left(\frac{T_w}{T_0}\right) - 4\right\}\frac{\theta}{M_e}\frac{dM_e}{dx} = \frac{C_{fe}}{2}. \tag{16a}$$

The skin-friction coefficient C_{fe} can be expressed in terms of θ using Eckert's reference enthalpy method. The details are given elsewhere (Stollery 1973) but the result is

$$\tfrac{1}{2}C_{fe} = A/\theta^{\frac{1}{4}} M_e^{\frac{3}{4}}, \tag{19}$$

where

$$A = \frac{0{\cdot}013 C_\infty^{\frac{1}{4}}}{(Re_x/x)^{\frac{1}{4}}(kM_\infty)^{\frac{3}{4}}}.$$

The 'constant' k comes from the definition of the reference temperature T^*, i.e.

$$\begin{aligned}\frac{T^*}{T_\infty} &= 0{\cdot}5\left[\left(1 + \frac{T_w}{T_0}\right) + \frac{M_\infty^2}{5}\left(0{\cdot}44r + \frac{T_w}{T_0}\right)\right]\\ &\simeq \frac{M_\infty^2}{5} 0{\cdot}5\left(0{\cdot}44r + \frac{T_w}{T_0}\right) \quad \text{for} \quad M_\infty^2 \gg 1\\ &= kM_\infty^2,\end{aligned}$$

where

$$k = 0{\cdot}04(1 + 2{\cdot}5T_w/T_0),$$

assuming that the recovery factor r is 0·9.

Substitution of (19) into (16a) enables the momentum equation to be re-arranged as

$$\theta^{\frac{1}{4}}\frac{d\theta}{dx} + B\frac{\theta^{\frac{5}{4}}}{M_e}\frac{dM_e}{dx} = \frac{A}{M_e^{\frac{3}{4}}}. \tag{20}$$

Provided that $B \equiv H_i(T_w/T_0) - 4$ is constant this equation is integrable to

$$\theta = \left(\frac{5A}{4}\right)^{\frac{4}{5}}\left[\int_0^x M_e^{\frac{1}{4}(5B-3)}\,dx\right]^{\frac{4}{5}} \Big/ M_e^B. \tag{21}$$

Noting that $\delta^* = H\theta$ and $P \simeq (M_\infty/M_e)^7$ for $\gamma = 1{\cdot}4$ and taking $H_i = 1{\cdot}3$ the final result is

$$\frac{M_\infty \delta^*}{x} = 0{\cdot}051\,\frac{1 + 1{\cdot}3T_w/T_0}{(1 + 2{\cdot}5T_w/T_0)^{\frac{3}{5}}}\left\{\frac{M_\infty^9 C_\infty}{Re_x}\right\}^{\frac{1}{5}}\frac{\left[\int_0^x P^\eta\,d\xi/x\right]^{\frac{4}{5}}}{P^\kappa}, \tag{22}$$

where $\eta = \frac{1}{7}(5{\cdot}75 - 1{\cdot}625T_w/T_0)$, $\kappa = \frac{1}{7}(6 - 1{\cdot}3T_w/T_0)$ and ξ is the dummy variable in x. If $P \simeq$ constant then (22) indicates that

$$\delta^*/x \sim \{C_\infty M_\infty^4/PRe_x\}^{\frac{1}{5}},$$

which is the relation derived in (3b). If $P = \text{constant} \times x^n$ is substituted in (22) to seek the strong viscous interaction solution (when $P \propto (d\delta^*/dx)^2$) the solution

$$P \sim (M_\infty^9 C_\infty/Re_x)^{\frac{2}{7}}$$

is obtained as in (6). As pointed out by one of the referees the complete solution of (22) for strong viscous interaction is of the form

$$P^{\frac{3}{4}} = C_1(M_\infty \delta^*)^{-\frac{1}{4}} + C_2(M_\infty \delta^*)^{\lambda},$$

where $\lambda = -\frac{5}{4}[21/(30-6{\cdot}5T_w/T_0)]$. The constant C_1 is known but C_2 is arbitrary. Putting $C_2 = 0$ gives the quoted result. The physical justification for this choice is that P must be finite (and less than the normal shock value) at $x = 0$. Hence the integral in (22) evaluated at $x = 0$ must be zero and so $C_2 = 0$.

The final result (22) indicates that the displacement thickness increases with the Mach number M_∞, decreases in an adverse pressure gradient and is almost independent of the wall temperature ratio T_w/T_0. The assumption that $H_i \simeq$ constant is reasonable provided that any adverse pressure gradient present is not so severe as to cause separation.

2.5. *Heat transfer and skin friction*

The expression already derived for θ [equation (21)] may be substituted back into (19) to obtain

$$M_\infty^3 St_e = M_\infty^3 \frac{C_{fe}}{2} = \frac{0{\cdot}204}{(1+2{\cdot}5T_w/T_0)^{\frac{3}{5}}} \left\{\frac{M_\infty^9 C_\infty}{Re_x}\right\}^{\frac{1}{5}} \frac{(M_\infty/M_e)^{\epsilon}}{\left[\int_0^x (M_\infty/M_e)^{\zeta}\, d\xi/x\right]^{\frac{1}{5}}}, \qquad (23)$$

where $\epsilon = \frac{1}{4}(7-1{\cdot}3T_w T_0)$ and $\zeta = \frac{1}{4}(23-6{\cdot}5T_w/T_0)$. To obtain St and C_f based on free-stream properties the above expression must be multiplied by ρ_e/ρ_∞. From the isentropic external flow assumption $\rho_e/\rho_\infty \simeq (M_\infty/M_e)^5 \simeq P^{\frac{5}{7}}$ hence

$$M_\infty^3 St_\infty = M_\infty^3 \frac{C_{f\infty}}{2} = \frac{0{\cdot}204}{(1+2{\cdot}5T_w/T_0)^{\frac{3}{5}}} \overline{\chi}_w \frac{P^{\sigma}}{\left[\int_0^x P^{\omega}\, d\xi/x\right]^{\frac{1}{5}}}. \qquad (24)$$

where $\sigma = \frac{1}{28}(27-1{\cdot}3T_w/T_0)$ and $\omega = \frac{1}{7}\zeta$. If $P =$ constant then $St_\infty \sim P^{\frac{4}{5}}$ as suggested earlier [see (13)]. Equation (24) suggests that both the Stanton number and the skin-friction coefficient decrease with Mach number and wall temperature ratio but increase with pressure gradient. These are the accepted trends except for near separation conditions, when $C_{f\infty}$ drops rapidly. It must be remembered that throughout this simple analysis flat-plate velocity profiles have been assumed.

3. Applications and discussion

As a simple illustrative example consider a flat plate at zero incidence. Even in the strong interaction zone near the leading edge P is a slowly varying function of x ($P \sim x^{-\frac{2}{7}}$, see (6)) and so the elementary expression (3 *b*) for δ^* might suffice.† With $y_w = 0$ equations (1 *a*), (2 *a*) and (3 *b*) may be combined as

$$y_e\left\{1+\gamma M_\infty^2 y_e'^2 \left[\frac{\gamma+1}{4} + \left\{\left(\frac{\gamma+1}{4}\right)^2 + \frac{1}{M_\infty^2 y_e'^2}\right\}^{\frac{1}{2}}\right]\right\}^{\frac{1}{5}} = a_1 x \left\{\frac{C_\infty M_\infty^4}{Re_x}\right\}^{\frac{1}{5}},$$

† The more general expression for δ^* [equation (22)] is always to be preferred on theoretical grounds. It is nevertheless true that the simpler relation [equation (3*b*)] intended mainly for illustrative purposes sometimes gives predictions in closer agreement with the experimental data.

where a_1 is now available from (22) for $\gamma = 1{\cdot}4$ as

$$a_1 = 0{\cdot}051 \frac{1+1{\cdot}3T_w/T_0}{(1+2{\cdot}5T_w/T_0)^{\frac{3}{5}}}. \tag{25}$$

The appropriate scaling is now

$$Y = M_\infty y/l, \quad X = x/l,$$

where
$$l = xM_\infty^9 C_\infty/Re_x.$$

The scaled equation is

$$Y_e \left\{1+\gamma Y_e'^2 \left[\frac{\gamma+1}{4} + \left\{\left(\frac{\gamma+1}{4}\right)^2 + \frac{1}{Y_e'^2}\right\}^{\frac{1}{2}}\right]\right\}^{\frac{1}{5}} = a_1 X^{\frac{4}{5}}. \tag{26}$$

Near the leading edge $Y_e'^2 \gg 1$ so the equation becomes

$$Y_e Y_e'^{\frac{2}{5}} = a_2 X^{\frac{4}{5}},$$

which has a solution

$$Y_e = (\tfrac{7}{6})^{\frac{2}{7}}_{2} a_2^{\frac{5}{7}} X^{\frac{6}{7}}, \tag{27}$$

where $a_2 = a_1/\{\frac{1}{2}\gamma(\gamma+1)\}^{\frac{1}{5}}$. The corresponding expression for P is

$$P = \{\tfrac{18}{49}\gamma(\gamma+1)\, a_1^2\}^{\frac{5}{7}} \overline{\chi}_s, \tag{28}$$

where $\gamma = 1{\cdot}4$.

Starting values for the computer solution of (26) may therefore be obtained from (27) and (28).† Further back on the plate $P \rightarrow 1$ and (26) shows that the boundary-layer growth reduces to the conventional flat-plate value $Y_e \sim X^{\frac{4}{5}}$.

The corresponding value of the Stanton number for strong interaction is given by (15) with the constant of proportionality taken from (24). Figure 1 shows P and St_∞ *vs.* X with the asymptotic value for large and small X marked.

Similar analyses to demonstrate the effects of turbulent viscous interaction on flow over flat plates at incidence and over concave and convex surfaces can easily be made still using the simplest expression for δ^*. Results are to be found in the thesis by Bates (1973).

3.1. *Flow past a wedge compression corner*

As mentioned in the introduction shock–boundary-layer interaction at a compression corner is probably the most important example of turbulent viscous interaction. In this case P varies rapidly near the corner and reaches high values over the ramp so the less approximate relation for $\delta^*(x)$ should be used. The problem then is to solve the set (1 *a*), (2 *a*) and (22),

$$P = 1+\gamma K^2 \left[\frac{\gamma+1}{4} + \left\{\left(\frac{\gamma+1}{4}\right)^2 + \frac{1}{K^2}\right\}^{\frac{1}{2}}\right],$$

where $K = M_\infty\, dy_e/dx$,

$$y_e = y_w + \delta^*$$

† Since the transition Reynolds number at high Mach numbers is so large there will be no region of turbulent strong viscous interaction. To apply the method a virtual origin must be defined and this was done in the experimental comparisons which follow, by using the relation $\Gamma \propto x^{\frac{4}{5}}$. The energy thickness Γ was found by integrating the measured heat-transfer-rate distribution over the flat-plate region.

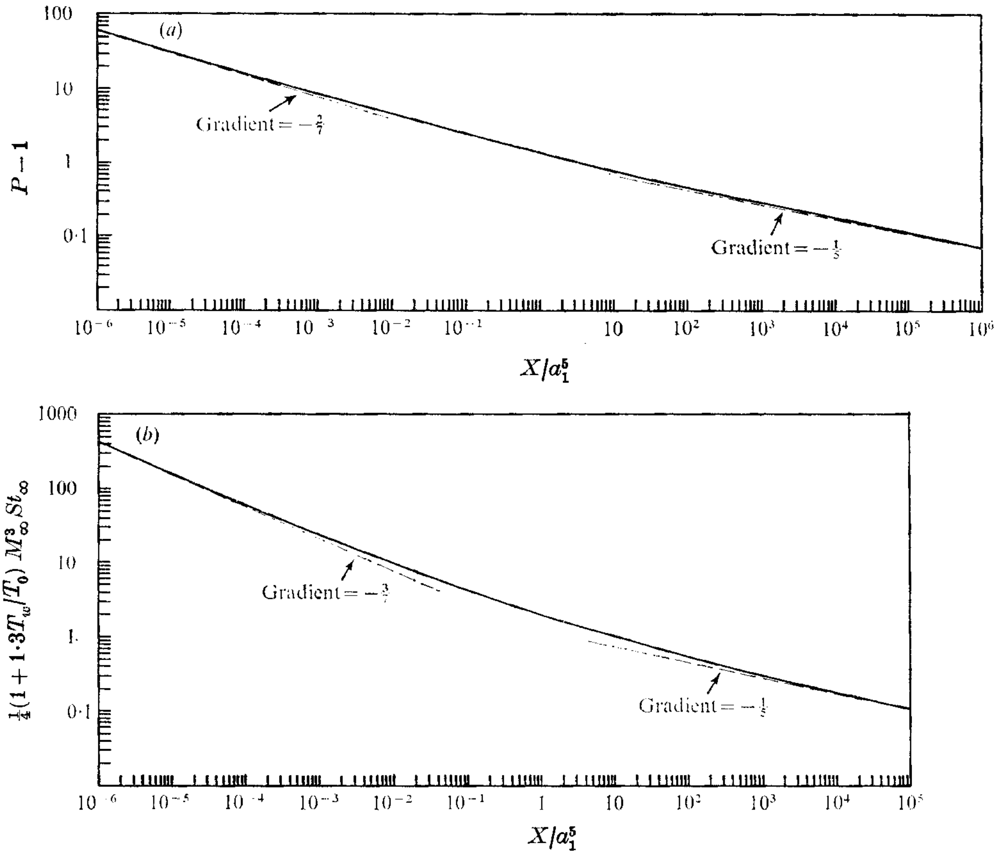

FIGURE 1. (*a*) Pressure distribution and (*b*) heat transfer on a flat plate at zero incidence. $X = \{Re_x/M_\infty^9\, C_\infty\}$.

and
$$\frac{M_\infty \delta^*}{x} = 0{\cdot}051\,\frac{1+1{\cdot}3T_w/T_0}{(1+2{\cdot}5T_w/T_0)^{\frac{5}{3}}}\,\overline{\chi}_w\,\frac{\left[\int_0^x P^\eta\, d\xi/x\right]^{\frac{4}{5}}}{P^\kappa},$$

where $\eta = \frac{1}{7}(5{\cdot}75 - 1{\cdot}625T_w/T_0)$ and $\kappa = \frac{1}{7}(6 - 1{\cdot}3T_w/T_0)$, for a given geometry y_w and initial conditions M_∞, unit *Re* and T_w/T_0. This set has been solved for hypersonic flow over a wedge compression corner under identical initial conditions to those used by Elfstrom (1972) and Coleman (1973) in their experiments. Comparisons between the theoretical predictions and experimental data are shown in figures 2 and 3. The heat-transfer estimates were made using (24) and the calculated pressure distribution $P(x)$.

For the 15° compression corner (figure 2) the agreement between theory and experiment is remarkably good considering the simplicity of the analysis. However, at 30° (figure 3) the agreement is not so good. The theoretical prediction of heat transfer rises above the experimental data to overestimate the values downstream on the wedge. This difference is probably due to the assumption of the isentropic edge flow conditions used in the boundary-layer analysis, an assumption which is grossly violated at the larger corner angles. Indeed the success of

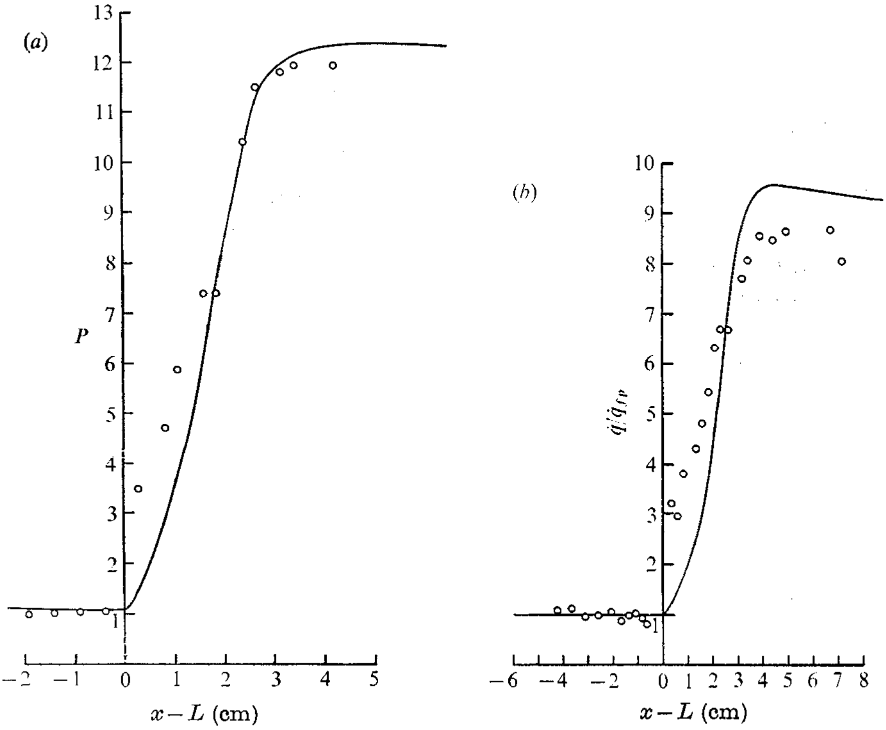

FIGURE 2. (*a*) Pressure distribution and (*b*) heat transfer on a wedge compression corner model. $M_\infty = 9{\cdot}22$, $\alpha = 15°$. Hingeline at $x = L$. $\dot{q}_{fp}$ = flat-plate heat transfer. —, theory; ○, data of Elfstrom *et al.*

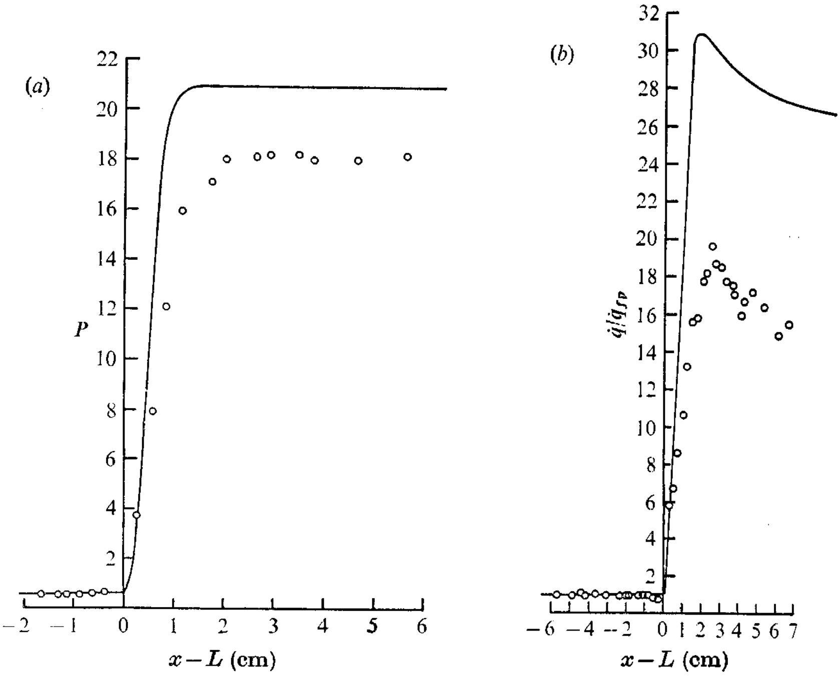

FIGURE 3. (*a*) Pressure distribution and (*b*) heat transfer on a wedge compression corner model. $M_\infty = 9{\cdot}22$, $\alpha = 30°$. Hingeline at $x = L$. $\dot{q}_{fp}$ = flat-plate heat transfer. —, theory; ○, data of Elfstrom *et al.*

the method in predicting the pressure for the larger angle model, and both pressure and heat transfer at the more modest turning angle, is due to the choice of the tangent-wedge rule for the pressure law. This is a reasonable approximation to the oblique shock relations and is the only way in which the true non-isentropic nature of the corner flow is taken into account. For concave and convex surfaces where the external flow would be isentropic the more appropriate Prandtl–Meyer relation should be used in place of the tangent-wedge rule. It would then be most interesting to compare the predictions of the modified method with data obtained from hypersonic turbulent flow over such shapes.

4. Incipient separation

We have demonstrated that the important parameters for strong viscous interaction at hypersonic speeds are $M_\infty^2\alpha^2$ and $\bar{\chi}_s$. Laminar-flow incipient-separation data are well correlated by these parameters, interpreting α as the incipient-separation value α_i and evaluating $\bar{\chi}_{\mathrm{Lam}}$, the laminar viscous interaction parameter, at the hinge line $x = L$. For turbulent flow similar reasoning would suggest that

$$M_\infty^2\alpha_i^2 \sim \{M_\infty^9 C_\infty/Re_L\}^{\frac{2}{7}}$$

or

$$\alpha_i \sim \{M_\infty^2 C_\infty/Re_L\}^{\frac{1}{7}}.$$

Reference to the compilation of experimental data given by Coleman & Stollery (1972) shows that the picture is far more complex. Certainly the values of α_i are much larger than those for laminar flow, where

$$\alpha_i \sim \{M_\infty^2 C_\infty/Re_L\}^{\frac{1}{4}},$$

but the only consistent trend shown by the experimental data is that α_i increases with the Mach number M_∞.

5. Laminar flow

As mentioned in the introduction Cheng *et al.* (1961) indicated the method of solution for all laminar viscous interaction problems. They used Lees's (1953) description of the hypersonic laminar boundary layer, in which he justifies neglect of the pressure-gradient term in the transformed momentum equation under cold-wall conditions, to obtain the simple relation

$$M_\infty \frac{\delta^*}{x} = 0{\cdot}664\left(\frac{\gamma-1}{2}\right)\left(1+2{\cdot}6\frac{T_w}{T_0}\right)\bar{\chi}_{\mathrm{Lam}}\left\{\int_0^x P\,d\xi/x\right\}^{\frac{1}{2}}\Big/P, \tag{29}$$

where $\bar{\chi}_{\mathrm{Lam}}$ is the laminar viscous interaction parameter $M_\infty^3(C_\infty/Re_x)^{\frac{1}{2}}$. Now the momentum integral equation is common to all types of boundary layer so the analysis presented here is immediately extendable to laminar flow. The only differences are that $H_i = 2{\cdot}6$ instead of $1{\cdot}3$ and

$$\frac{C_{fe}}{2} = \left\{0{\cdot}221\frac{C_\infty}{M_\infty^3 Re_x/x}\right\}\frac{M_e^3}{\theta}. \tag{30}$$

This latter result is obtained by applying Eckert's reference enthalpy method to the local incompressible value taken as

$$\tfrac{1}{2}C_{fi} = 0{\cdot}332 Re_x^{-\frac{1}{2}} = 0{\cdot}221 Re_\theta^{-1}.$$

Substitution of these relations leads to the final expression

$$\frac{M_\infty \delta^*}{x} = 0{\cdot}664\left(\frac{\gamma-1}{2}\right)\left(1+2{\cdot}6\frac{T_w}{T_0}\right)\bar{\chi}_{\mathrm{Lam}}\frac{\left\{\int P^\phi\, d\xi/x\right\}^{\frac{1}{2}}}{P^\psi}, \tag{31}$$

where $\phi = \frac{1}{7}(5-5{\cdot}2T_w/T_0)$ and $\psi = \frac{1}{7}(6-2{\cdot}6T_w/T_0)$, which is very similar to Lees's result (29) though making somewhat different assumptions and derived in a different way. In fact the predictions of laminar viscous interaction on a flat plate from (31) agree very well with those made using the improvement to Lees's analysis suggested by Moore (1961).

6. Axisymmetric flow

The extension to axisymmetric flow is perfectly straightforward. The momentum integral equation is

$$\frac{d\theta}{dx} + (H+2-M_e^2)\frac{\theta}{u_e}\frac{du_e}{dx} + \frac{\theta}{r}\frac{dr}{dx} = \frac{C_f}{2}. \tag{32}$$

Once again this equation is directly integrable assuming that H_i and T_w/T_0 are constant. Taking the same expression for the local skin friction and form parameter as in two-dimensional flow the result for a turbulent boundary layer is

$$\frac{M_\infty \delta^*}{x} = \frac{0{\cdot}051(1+1{\cdot}3T_w/T_0)}{(1+2{\cdot}5T_w/T_0)^{\frac{3}{5}}}\left\{\frac{M_\infty^9 C_\infty}{Re_x}\right\}^{\frac{1}{5}}\frac{\left[\int_0^x P^\eta r^{\frac{5}{4}}\, d\xi/x\right]^{\frac{4}{5}}}{P^\kappa r}, \tag{33}$$

where $\eta = \frac{1}{7}(5{\cdot}75-1{\cdot}625T_w/T_0)$ and $\kappa = \frac{1}{7}(6-1{\cdot}3T_w/T_0)$. The tangent-cone rule could be used in place of the tangent-wedge relation for pressure but again the choice must be guided by the shape of body in question.

7. Conclusions

The problem of turbulent viscous interaction at hypersonic speeds may be tackled in a similar way to that described by Cheng *et al.* (1961) for laminar flow. The important parameters describing the effects of shape and displacement are $M_\infty \alpha$ and $(M_\infty^9 C_\infty/Re_x)^{\frac{1}{5}}$ for weak interaction and $M_\infty^2 \alpha^2$ and $(M_\infty^9 C_\infty/Re_x)^{\frac{2}{7}}$ for strong interaction.

The growth of the boundary-layer displacement thickness $\delta^*(x)$ in an unknown pressure gradient for any given Mach number and wall temperature ratio can be found by modifying Spence's solution of the momentum integral equation. Using this expression for δ together with suitable laws relating the pressure to the effective shape the equations may be solved simultaneously to give δ^*, P and hence the heat-transfer rate. The method has been tested against some experimental data at $M_\infty = 9$ with promising results.

The authors would like to acknowledge the encouragement provided by the critical comments of Dr J. E. Green (RAE), Mr P. Bradshaw (Imperial College) and Professor P. Libby whilst on leave from the University of California, La Jolla.

REFERENCES

Barnes, J. W. & Tang, H. H. 1966 *A.I.A.A. J.* **4**, 1838.

Bates, L. 1973 Ph.D. thesis, Imperial College, London.

Cheng, H. K., Hall, J. G., Golian, T. C. & Hertzberg, A. 1961 *J. Aero. Sci.* **28**, 353.

Coleman, G. T. 1973 Ph.D. thesis, Imperial College, London.

Coleman, G. T. & Stollery, J. L. 1972 *J. Fluid Mech.* **56**, 741.

Duncan, W. J., Thom, A. S. & Young, A. D. 1970 *Mechanics of Fluids*. London: Edward Arnold.

Eckert, E. R. G. 1956 *Trans. A.S.M.E.* **78**, 1273.

Elfstrom, G. W. 1972 *J. Fluid Mech.* **53**, 113.

Hayes, W. D. & Probstein, R. F. 1959 *Hypersonic Flow Theory*. Academic.

Lees, L. 1953 *J. Aero. Sci.* **20**, 143.

Moore, F. K. 1961 *J. Aero Sci.* **10**, 753.

Spence, D. A. 1961 *Aero. Res. Counc. R. & M.* no. 3191.

Stollery, J. L. 1970 *J. Fluid Mech.* **43**, 497.

Stollery, J. L. 1973 *Imperial College Aero. Rep.* no. 73-04.

Sullivan, P. A. 1970 *A.I.A.A. J.* **8**, 765.

Young, A. D. 1953 *Aero. Res. Counc. Paper*, no. 15970.